



Latin American Journal of Energy Research – Lajer (2024) v. 11, n. 1, pp. 45–56  
<https://doi.org/10.21712/lajer.2024.v11.n1.p45-56>

## Fluidodinâmica e segregação da mistura de areia e resíduo de malte em leito de jorro cônico

### *Fluid dynamics and segregation of sand-malt waste mixture in conical spouted bed*

Natália P. Almeida<sup>1</sup>, Taísa S. Lira<sup>2</sup>, Beatriz C. Silvério<sup>3,\*</sup>, José L. Vieira Neto<sup>3</sup>, Kássia G. Santos<sup>3</sup>

<sup>1</sup>Aluna do Programa de Pós-Graduação em Engenharia Química, Universidade Federal de Uberlândia – UFU, Brasil

<sup>2</sup> Professor da Universidade Federal do Espírito Santo – Ufes, campus São Mateus, ES, Brasil

<sup>3</sup> Professor da Universidade Federal do Triângulo Mineiro – UFTM, ICTE, campus Univerdecidade, MG, Brasil

\*Autor para correspondência, E-mail: [beatriz.silverio@uftm.edu.br](mailto:beatriz.silverio@uftm.edu.br)

Received: 12 March 2024 | Accepted: 23 May 2024 | Published online: 5 June 2024

**Resumo:** Um dos setores mais tradicionais do agronegócio brasileiro é a indústria cervejeira. O cereal mais utilizado nesse processo é a cevada, gerando como principal subproduto resíduo de malte, uma biomassa lignocelulósica. A pirólise em leito de jorro é uma tecnologia promissora para geração de energia renovável a partir de resíduos agroindustriais. Assim, para verificar a possibilidade de aplicação do leito de jorro como um reator de pirólise, foram realizadas análises fluidodinâmicas da mistura de resíduo de malte e areia. Observou-se como a altura estática do leito e a fração de massa da biomassa influenciam a condição de jorro mínimo e crítico, e a segregação das partículas. As correlações analisadas apresentaram bons resultados na previsão da velocidade mínima de jorro, com um erro relativo de 4,83%. Para a queda de pressão máxima, a melhor correlação mostrou um erro relativo de 13,91% e, para a queda de pressão do jorro mínimo, um erro relativo de 5,45%. Também, em relação à segregação foi observado que a base do leito apresentou taxas mais elevadas de segregação, com uma maior presença de partículas de areia.

Palavras-chave: Leito de jorro, segregação de partículas em leito de jorro, segregação de partículas, resíduo de malte, mistura de partículas.

**Abstract:** One of the most traditional sectors of Brazilian agribusiness is the brewing industry. The most used cereal in this process is barley, generating as the main by-product malt waste, a biomass called lignocellulosic. The pyrolysis in spouted bed is a promising technology for renewable energy generation through agro-industrial wastes. Thus, aiming at contributing to the application of the spouted bed as a pyrolysis reactor, the fluid dynamic analyzes of the mixture of malt waste and, sand was carried out. It was observed how the static bed height and biomass mass fraction influence the condition of minimum and critical spout and the segregation of the particles. The correlations analyzed presented good results to predict the minimum spout velocity, with a relative error of 4.83%. For the maximum pressure drop, the best correlation showed relative error of 13.91% and, for pressure drop of minimum spout, a relative error of 5.45%. It was also observed that the base of the bed showed higher segregation rates, with a higher presence of sand particles.

Keywords: spouted bed particle segregation, brewer's spent grain, malt waste, particle mixing, particle segregation.

## 1 Introduction

One of the most traditional sectors of the Brazilian agribusiness is the brewer industry, with the productive chain responsible for 1.6% of GDP and 14% of the national processing industry (CERVBRASIL, 2020). The most widely used cereal in this process is barley and, consequently, barley malt waste is the main residue of the brewing industry.

According to Cordeiro, El-Aouar and Gusmão (2013) malt waste is a biomass resulting from the wort filtration process, consisting of bark and, pulp residues from the grains, mixed, suspended or dissolved in the wort. Hence, the beer industry stands out, which due to the rich composition of its residues has relevant potential for application in bioprocesses Mathias, Mello and Servulo (2014). It is produced 14 to 20 kg of malt waste per 100 liters of beer produced, which characterizes this waste quantitatively as the main by-product of the brewing process.

According to Libardi et al. (2016), biomass pyrolysis is considered one of the most promising process to obtain renewable energy. The thermal decomposition of a solid material occurs in the total or partial absence of oxygen, generating products with high calorific value, such as char, bio-oil and, pyrolytic gas.

Thus, it is essential to choose equipment, such as a pyrolysis reactor, that efficiently promotes contact between the fluid and, the particle (Shao et al., 2014). A conventional gas-solid spouted bed generally consists of a vertical cylindrical connected with a conic part, and the literature presents fluid dynamic studies of the different variations of this bed (Shao et al., 2014; Araújo and Santos, 2017). Several studies were carried out by this research group with the aim to evaluate the kinetics of degradation of different biomasses for pyrolysis, as well as for the evaluation of the fluid dynamics of different materials in the spouted bed (Silvério et al., 2017; Batista et al., 2017; Santos et al., 2012a; Santos et al., 2012b; Santos et al., 2013a).

Particle mixing experiments in spouted bed help to understand the segregation mechanisms of the equipment. The study of the fluid dynamics of the mixture of biomass and, inert in the spouted bed is important because it interferes directly in the yield and, final composition of the products obtained by pyrolysis. (Santos, 2012; Barcelos et al., 2020; Santos et al., 2015; Santos et al., 2017).

Conical spouted beds have become a promising technique for many processes involving particle mixtures, such as drying, coating, granulation and pyrolysis (Barrozo et al., 2019; Barcelos et al., 2020; Santos et al., 2013b; Santos et al., 2019; Shu et al., 2014; Bai et al., 1996; Santos et al., 2013c). Over the years, there was some studies about mixing and, segregation on spouted and, fluidized bed. Bancelos and Freire (2006) conical spouted bed showed more restrictive in operating with particle mixtures than those reported by San José et al. (1994).

The literature emphasized that the larger and, denser particles present less recirculation time, since they follow a shorter trajectory within the bed (Santos, 2012; Santos et al., 2019). Thus, when entrained by air in the spout region, they rise to a smaller height at the fountain and, fall further away from the wall, in a more internal annular position. In addition, it was concluded that the main factor that promotes segregation is particle mirroring, a phenomenon that occurs in the fountain region, and, which is more pronounced for smaller and, less dense particles than for larger particles.

Barcelos et al. (2020) studied the mechanisms of particle segregation in a spouted bed operating with binary mixtures and, concluded that the segregation of particles with biomass and, sand mixtures was more pronounced at the base of the apparatus, with a prevalence of sand, because it is denser. Segregation was subtle in the other regions of the bed and, Araújo and Santos, (2017) found that segregation was more pronounced in biomass-rich mixtures when sugarcane waste was used.

A literature study presents the effect of the particle density on the mixing and, segregation behavior in a spout-fluid bed and, concluded that a monotonic increase in the spouting or fluidizing gas velocity is not necessary to promote mixing (Zhang et al., 2012). In addition, the study concluded that the location of the transition region for a binary mixture with different densities is different from one for a binary mixture with different sizes. Other fluid dynamic studies were conducted for the purpose to evaluate better conditions of mixture of particles in spouted bed (Barrozo et al., 2019; Santos et al., 2015; Santos et al., 2019; Shu et al., 2014).

In this context, the aim of this study was to analyze the fluid dynamics behavior of a binary mixture containing malt waste and, sand in the conical spouted bed. Another aim was to evaluate how the height of the static bed and, the mass fraction of biomass influence the velocity and, pressure drop of minimum spout and, the segregation of particles. A study on the applicability of several correlations proposed in the literature was also carried out to calculate maximum pressure drops, velocity and, pressure drop of minimum spout for the mixture under analyzes.

## 2 Materials and methods

### 2.1 Experimental apparatus

The experimental configuration used to acquire the data discussed in this study was composed by a spouted bed with cylindrical section diameter of 0.20 m and an inner inlet orifice diameter of 0.044 m. Table 1 shows the spouted bed geometry and, particles properties used in this study: sand (S) and, malt waste (MW) particles.

The conical base of the spouted bed reactor was modified by inserting a guillotine sampler to enable sampling of the mixture at different axial positions in the bed. The guillotines were placed 2 cm away from each other. Thus, the first guillotine (lower axial position) was 2 cm away from the bottom of the bed. Air was supplied using an IBRAM centrifugal blower (2.0 hp). The air flow rate was measured by a digital rotameter, while the pressure drop was measured using and, a pressure transducer (Dwyer brand, model 616C-4, operating in a range of 0 – 20 inches of water), where the signal was transmitted to a microcomputer by an A/D data acquisition card (PCI-6021E from National Instruments) and, processed by LabVIEW™ 7.1 software. Data were sampled for 10.24 s at a sampling frequency of 100 Hz.

Table 1. Operating conditions and properties of the particles used in the spouted bed experiments.

Spouted bed geometry		
$D_c$ (m)	Cylinder Diameter	0.200
$D_0$ (m)	Inlet Diameter	0.044
$H_c$ (m)	Conical height	0.200
$H$ (m)	Height of cylindrical part	0.395
$\gamma$	Cone angle	60°
Particle Proprieties		
$\rho_b$ (kg/m <sup>3</sup> )	Bulk density of biomass	2480
$\rho_i$ (kg/m <sup>3</sup> )	Bulk density of inert	1140.47
$d_b$ (m)	Particle inert diameter	$2.4 \cdot 10^{-3}$
$d_i$ (m)	Particle diameter	$1.29 \cdot 10^{-3}$
$\phi_b$	Inert sphericity	0.342
$\phi_i$	Biomass sphericity	0.800
Bed Voidage		
$\varepsilon_0$	Bed voidage for $X_b=0.1$	0.525
$\varepsilon_0$	Bed voidage for $X_b=0.3$	0.648
$\varepsilon_0$	Bed voidage for $X_b=0.5$	0.721

### 2.2 Fluid dynamics experiments

Characteristic curves were obtained by plotting the spout pressure drop as a function of decreasing inlet air velocity and, visually monitoring the movement of particles on the bed surface. The minimum spouting condition is usually defined as the point at which the spout collapses. The characteristic experimental curves were obtained in duplicate.

Fluid dynamics and, segregation tests were performed using a factorial experimental design (3<sup>2</sup>) to investigate the effect of the initial mass fraction of biomass in the mixture ( $X_b = 0.1, 0.3, \text{ and } 0.5$ ) and, static bed height ( $H_0 = 0.06, 0.08, \text{ and } 0.10$  m) on the following responses: minimum spouting condition (air flow rate ( $q_{ms}$ ) and, pressure drop  $-\Delta P$ ), maximum pressure drop ( $-\Delta P_{ms}$ ), and mixing index ( $I_M$ ). Eqs (1) and, (2) present the coded variables,  $x_1$  and  $x_2$ , which correspond to the initial mass fraction of biomass and, static bed height, respectively.

$$x_1 = \frac{X_b - 0.3}{0.2} \quad (1)$$

$$x_2 = \frac{H_0 - 0.08}{0.02} \quad (2)$$

According to the composition of each mixture, the masses of the particles were determined, homogenized and, added to the spouted bed until the static bed height of the reference test was reached.

The bed height, particle densities and, mass balance in the bed were used to determine the static bed voidage. The entire set of experimental data was comprehensively analyzed using multiple regression, and the significance of regression parameters was analyzed using the Student's t test. All statistical tests are performed with a significance level of 10%.

### 2.3 Prediction of fluid dynamics parameters by empirical correlation

The literature has some correlations to predict the minimum spout velocity ( $q_{ms}$ ), from the Archimedes (Ar) and, Reynolds number in the minimum spout ( $Re_{ms}$ ), its corresponding pressure drop ( $-\Delta P_{ms}$ ) and the maximum pressure drop ( $-\Delta P_{max}$ ). These models generally comprise the interference of geometric factors, particle properties and, initial process conditions. The diameters and, densities of the particles used in the binary system were defined according to three different definitions of effective particle diameter ( $d_{eff}$ ) and, specific effective mass ( $\rho_{eff}$ ).

Table 2 summarizes the empirical correlations (Eq (9) to (23)) used to predict the air velocity and, pressure drop at the minimum spout condition, as well the maximum pressure drop in the bed.

Table 2. Empirical correlations in the minimum spout and maximum pressure drop in the bed<sup>[37,38]</sup>.

References	Correlations	Boundary Conditions
Gorshtein and Muklenov Olazar et al. (1992;1993;2006)	$(Re)_{jm} = 0.174 Ar^{0.5} \left(\frac{D_b}{D_0}\right)^{0.85} \operatorname{tg}\left(\frac{\gamma}{2}\right)^{-1.25}$ (9)	$H_0=3-15\text{cm}; H_0/D_0 = 1.3-8.5;$ $\gamma = 12-60^\circ; d_p=0.5-2.5 \text{ mm};$ $\rho_s = 980-2360 \text{ kg/m}^3$
Muklenov and Gorshtein Olazar et al. (1992;1993;2006)	$(Re)_{jm} = 3.32 Ar^{0.33} \left(\frac{H_0}{D_0}\right) \operatorname{tg}\left(\frac{\gamma}{2}\right)^{0.55}$ (10) $\frac{-\Delta P_{jm}}{H_0 \rho_b g} = 7.68 \left[\operatorname{tg}\left(\frac{\gamma}{2}\right)\right]^{-0.2} (Re)_{jm}^{-0.2} \left(\frac{H_0}{D_0}\right)^{-0.33}$ (11)	$D_0=10.3-12.9 \text{ mm}; H_0=3-15 \text{ cm};$ $\gamma=12-60^\circ; d_p=0.5-2.50 \text{ mm};$ $\rho_s=1000-2360 \text{ kg/m}^3; D_c= 5 \text{ cm}.$
Goltsiker Gobordhan Patro, (2007)	$(Re)_{jm} = 0.73 Ar^{0.14} \left(\frac{H_0}{D_0}\right)^{0.9} \left(\frac{\rho_{eff}}{\rho}\right)^{0.47}$ (12)	$D_0=0.41-1.23 \text{ cm}; H_0=5-31 \text{ cm};$ $\gamma=26-60^\circ; d_p=0.5-2.5 \text{ mm};$ $\rho_s = 800-1630 \text{ kg/m}^3.$
Tsvik et al. (1967)	$(Re)_{jm} = 0.4 Ar^{0.52} \left(\frac{H_0}{D_0}\right)^{1.24} \operatorname{tg}\left(\frac{\gamma}{2}\right)^{0.42}$ (13)	$D_0=2-4 \text{ cm}; H_0=10-50 \text{ cm};$ $H_0/D_0 = 1.6-8.7; \gamma=20-50^\circ;$ $d_p=1.5-4.0 \text{ mm};$ $\rho_s = 1650-1700 \text{ kg/m}^3.$
Olazar et al. (1992;1993;2006)	$(Re)_{jm} = 0.126 Ar^{0.5} \left(\frac{D_b}{D_0}\right)^{1.68} \operatorname{tg}\left(\frac{\gamma}{2}\right)^{-0.57}$ (14) $\frac{-\Delta P_{max}}{H_0 \rho_{eff} (1-\varepsilon_0) g} = 1.2 \operatorname{tg}\left(\frac{\gamma}{2}\right)^{-0.11} (Re)_{jm}^{-0.06} \left(\frac{H_0}{D_0}\right)^{0.08}$ (15) $\frac{-\Delta P_{jm}}{-\Delta P_{max}} = 1 + 0.116 \left(\frac{H_0}{D_0}\right)^{0.50} \operatorname{tg}\left(\frac{\gamma}{2}\right)^{-0.8} Ar^{0.0125}$ (16)	$D_0=3-6 \text{ cm}; H_0=3.6-6.1 \text{ cm};$ $\gamma=28-45^\circ; d_p=1-2.5 \text{ mm};$ $\rho_s = 240-3520 \text{ kg/m}^3.$
Pallai and Nemeth (1969)	$-\Delta P_{max} = H_0 (\rho_{eff}-\rho)(1-\varepsilon) g$ (17) $\frac{-\Delta P_{jm}}{-\Delta P_{max}} = 0.8 - 0.01 \frac{D_c}{D_0}$ (18)	$D_c = 10 \text{ a } 30 \text{ cm}.$
Sampaio Olazar et al. (1992;1993;2006)	$-\Delta P_{jm} = \frac{2}{3} \rho_b g H_0$ (19)	$D_0=15\text{cm}; H_0=3-15 \text{ cm};$ $\gamma= 60^\circ; d_p=4-6 \text{ mm};$ $\rho_s = 1100-1190 \text{ kg/m}^3.$
Olazar et al. (1992;1993;2006)	$\frac{-\Delta P_{jm}}{-\Delta P_{max}} = \left[1 + 0.35 \left(\frac{ H_0-H_c }{D_c}\right) \left(\frac{D_c}{D_0}\right)^{1.1} Ar^{0.1}\right]^{-1}$ (20)	$H_0 < 35 \text{ cm}; \rho_p = 2420 \text{ kg/m}^3.$
Saldarriaga et al. (2017)	$\frac{-\Delta P_{max}}{H_0 \rho_{eff} (1-\varepsilon_0) g} = 1.20 \operatorname{tg}\left(\frac{\gamma}{2}\right)^{-0.11} (Re)_{jm}^{-0.06} \left(\frac{H_0}{D_0}\right)^{0.3}$ (21)	$0.83 < H_0/D_0 < 50; 0.25 < \operatorname{tg}\left(\frac{\gamma}{2}\right) < 0.41$ $50 < (Re)_{jm} < 4900.$
Reynolds Number (Re)	$(Re)_{jm} = \frac{q_{jm} \rho d_{eff}}{\mu}$ (22)	Arquimedes Number (Ar) $Ar = \frac{\rho d_{eff}^3 (\rho_{eff}-\rho)}{\mu^2}$ (23)

The definition of Goossens and Dumont (Gobordhan Patro, 2007) considers the mass fractions of the components of the mixture studied and, their individual specific and, total effective masses when calculating the effective diameter, as shown by the Eq (3) and, (4).

$$\frac{1}{\rho_{\text{eff}}} = \frac{(1 - X_b)}{\rho_i} + \frac{X_b}{\rho_b} \quad (3)$$

$$\frac{1}{d_{\text{eff}}\rho_{\text{eff}}} = \frac{(1 - X_b)}{\rho_i d_i} + \frac{X_b}{\rho_b d_b} \quad (4)$$

The definition of Bai et al. (1996) considers only the individual diameters and, mass fractions of the mixture in the calculation of the effective diameter, as shown in Eq (5) and, (6).

$$\rho_{\text{eff}} = \frac{1}{\frac{(1 - X_b)}{\rho_i} + \frac{X_b}{\rho_b}} \quad (5)$$

$$d_{\text{eff}} = \frac{1}{\frac{(1 - X_b)}{d_i} + \frac{X_b}{d_b}} \quad (6)$$

Asif (2010) considers the individual volumetric fractions in the calculation of the effective diameter, the sphericities and, diameters of the particles, through the Eq (7) and, (8).

$$\rho_{\text{eff}} = X_{v,i}\rho_i + X_{v,b}\rho_b \quad (7)$$

$$\frac{1}{d_{\text{eff}}} = \left[ \left( \frac{X_{v,i}}{\phi_i d_i} \right) + \left( \frac{X_{v,b}}{\phi_b d_b} \right) \right] \quad (8)$$

## 2.4 Particle segregation

The particulate material was kept in a spout regime at a velocity of 20% greater than the minimum flow rate for 5 minutes. Thereafter, the blower was suddenly switched off and, the guillotines were inserted to divide the material into a set of five samples at different axial positions (Santos et al., 2013b). Then, biomass and sand particles were separated. The average mass fractions of biomass were calculated for the axial positions as 0.01, 0.03, 0.05, 0.07, and, 0.09 m.

The mixing index ( $I_M$ ) expresses the degree of segregation and, can be defined as the ratio between the biomass mass fraction in compartment  $i$  ( $X_{bi}$ ) and the initial MW mass fraction in the bed ( $X_{b0}$ ). Hence, if  $I_M > 1$ , MW particles are concentrated in the compartment; if  $I_M < 1$ , sand particles are in higher concentration and, if  $I_M = 1$ , there is no marked particle segregation, and, the concentration of the mixture remains unchanged. The effect of factors  $x_1$  and,  $x_2$  on particle segregation was evaluated using the mixing index at the bed top ( $I_{M-t}$ ) and, bottom ( $I_{M-b}$ ).

## 3 Results and discussion

### 3.1 Characteristic curves

The spouting regime was achieved in all experimental conditions carried out, which indicates that S-MW mixtures with 10-50 wt% of MW are suitable for performing the pyrolysis in this spouted bed.

Figure 2 presents the characteristic curve of the pressure drop as a function of air velocity and, identify the minimum spouting condition for a spouted bed operating with a S-MW mixture with  $X_b = 0.3$  and,  $H_0 = 0.08$  m. Through the characteristic's curves, all spouting conditions have been identified.

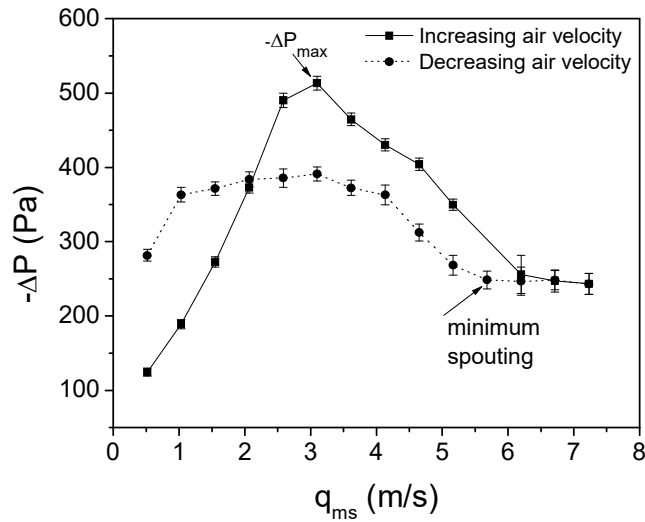


Figure 2. Characteristic curve obtained for  $X_b = 0.3$  and  $H_0 = 8$  cm. Source: Pazin et al. (2024)

Table 3 displays the air velocities for the minimum spout flow rate ( $q_{ms}$  (m/s)), and, experimental pressure drops ( $-\Delta P_{ms}$  (Pa)) relative to the minimum spout of each mixture composition analyzed, as well the maximum pressure drops ( $-\Delta P_{max}$  (Pa)).

Table 3. Results of maximum pressure drop, minimum spout velocity and pressure condition.

Run	Factors		Fluid dynamic results			Segregation	
	$X_b$ ( $x_1$ )	$H_0$ ( $x_2$ )	$q_{ms}$	$-\Delta P_{ms}$	$-\Delta P_{max}$	$I_{M-t}$	$I_{M-b}$
1	0.1 (-1)	0.06 (-1)	4.65	385.47	549.75	1.125	0.610
2	0.1 (-1)	0.08 (0)	5.68	500.68	1078.83	1.119	0.606
3	0.1 (-1)	0.10 (+1)	7.23	592.73	1587.23	1.218	0.546
4	0.3 (0)	0.06 (-1)	4.13	229.40	388.65	1.313	0.489
5	0.3 (0)	0.08 (0)	5.68	248.54	513.18	1.300	0.448
6	0.3 (0)	0.10 (+1)	7.23	278.91	555.11	1.256	0.417
7	0.5 (+1)	0.06 (-1)	4.18	168.33	276.86	1.312	0.430
8	0.5 (+1)	0.08 (0)	5.17	189.39	323.80	1.267	0.493
9	0.5 (+1)	0.10 (+1)	6.20	209.88	557.70	1.201	0.491

### 3.2 Effect of factors on spouted bed fluid dynamics of MW-S mixture

Eq (24) represents the minimum spout air velocity as a function of the coded factors, with a square correlation coefficient  $R^2 = 0.964$ . Residuals were random and, normally distributed. It is possible to observe that only the variables in the isolated form had a significant effect on the response. The effect of static bed height directly influences the minimum spout velocity, since an increase in height causes an increase in the total mass of the mixture, and consequently, the necessary airflow to establish the spout. On the other hand, the increase in the mass fraction of malt cake decreases the air velocity needed to establish the spout. This occurs because a higher fraction of the lighter component makes the density of the mixture lower, decreasing the resistive force, and consequently the air velocity in the minimum spout.

$$q_{ms} = 5.572 - 0.335x_1 + 1.283x_2 \quad (24)$$

The pressure drop in the minimum spouting condition can be predicted by Eq (25) ( $R^2 = 0.989$ ), while maximum pressure drop is described by Eq (26), with  $R^2 = 0.938$ . In both equations, it can be seen that biomass mass fraction influenced the pressure drop by the linear and, quadratic terms. Mixtures rich in biomass are lighter and, offer lower resistance to airflow, so, and, increase of  $X_b$  led to a reduction of  $-\Delta P_{ms}$  and,  $-\Delta P_{max}$ . On the other side, an increase of static bed height led to higher pressure drops, due to the higher amount of particles in the mixture.

$$-\Delta P_{ms} = 252.283 - 151.88x_1 + 49.720x_2 + 88.7970x_1^2 - 41.428x_1x_2 \quad (25)$$

$$-\Delta P_{\max} = 485.647 - 342.908x_1 + 247.46x_2 + 243.382x_1^2 - 189.16x_1x_2 \quad (26)$$

Figure 3 presents the response surfaces for the air velocity in the minimum spout (Figure 3A), pressure drop in the minimum spouting (Figure 3B) and, maximum pressure drop (Figure 3C).

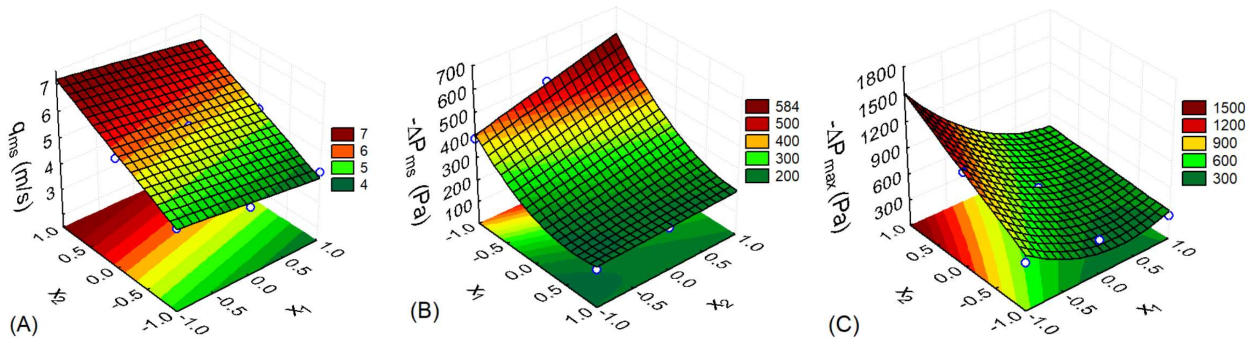


Figure 3. Response surface as a function of the mass fraction of biomass and the height of the static bed, for: (A) air velocity in the condition of minimum spout; (B) pressure drop in the condition of minimum spout; (B) maximum pressure drop.

### 3.3 Fluid dynamics prediction by empirical correlations

The correlations found in the literature for the prediction of minimum spout velocity, minimum spout pressure drop, and, maximum pressure drop were proposed for regular materials and, do not account for specific biomass characteristics, such as low sphericity. Once the biomass-sand mixtures have a complex particle dynamic in spouted beds, some correlations did not present satisfactory results. Among the three definitions of effective particle diameter ( $d_{\text{eff}}$ ) and, specific effective mass ( $\rho_{\text{eff}}$ ) studied, the Bai et al., (1996) approach was the one which showed the lowest deviations. It is possible to notice in Table 4, that the definition of the effective properties only significantly affects the prediction of  $q_{\text{ms}}$ , but does not present a considerable effect in the prediction of  $-\Delta P_{\text{ms}}$  and,  $-\Delta P_{\text{max}}$ . This fact was already expected, since the Archimedes number has exponents that are more significant in these correlations, having, in this way, greater influence on the calculation of  $q_{\text{ms}}$ . Besides, the Archimedes number is the parameter that most influenced by the definition of the effective properties, since the effective diameter appears cubed in his calculation.

Figure 4 to 6 presents the comparison between experimental data and, simulated values of  $q_{\text{ms}}$  (Figure 4),  $-\Delta P_{\text{ms}}$  (Figure 5) and  $-\Delta P_{\text{max}}$  (Figure 6), using the Bai et al. (1996) approach.

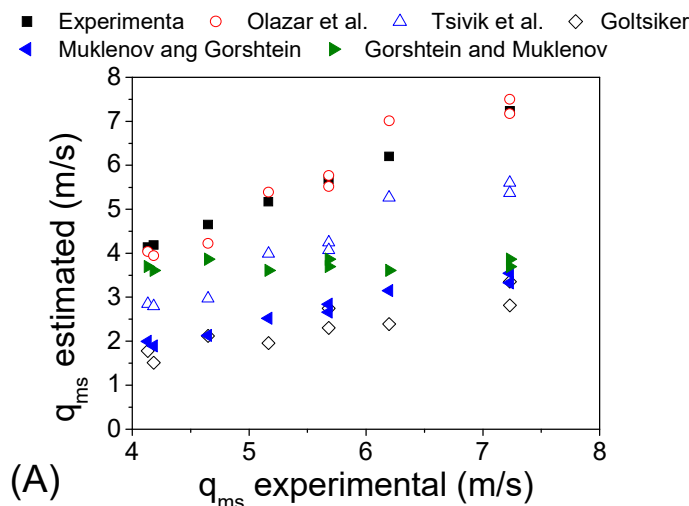


Figure 4. Comparison between minimum spouting velocities experimental and estimated data, using Bai et al. (1996).

Olazar et al. (2006) observed that for fine particles, with  $d_p$  between 0.3 and, 0.8 mm, the effective diameter correlation proposed by Bai et al. (1996) is satisfactory, while the definition of effective diameter proposed by Goossens et al. (1971) is recommended for coarse particles, with  $d_p$  between 0.8 and, 4.0 mm. However, for minimum spout velocity, the use of Bai et al. (1996) to calculate the effective properties better

adjusted some of the correlations studied, despite the results obtained by the definition of Goossens et al. (1971) also present satisfactory results.

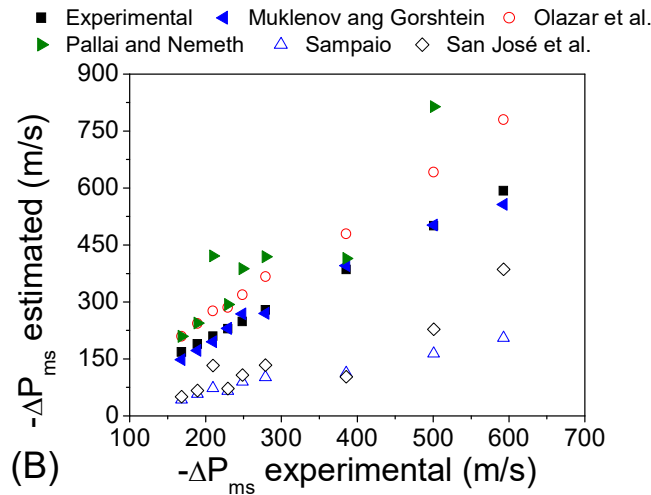


Figure 5. Comparison between pressure drop at minimum spouting experimental and estimated data, using Bai et al. (1996).

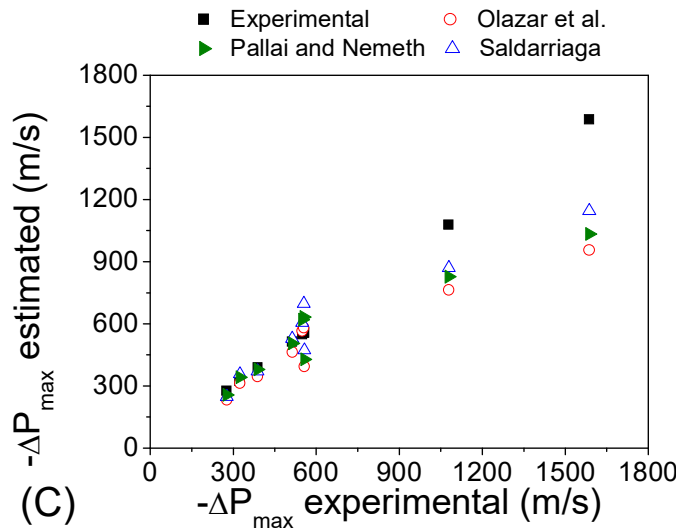


Figure 6. Comparison between maximum pressure drop experimental and estimated data, using Bai et al. (1996).

The correlation that best represented the experimental data for  $q_{ms}$  was that of Olazar et al. (1992) as shown by Figure 4. The relative error of 4.83% from Olazar et al. (1993) correlation suggests that is satisfactory for predicting the minimum spout velocity of the MW-S mixture when associated to Bai et al. (1996) definition. This model is suitable for moderately deep beds ( $H_0/D_c = 1$  to 2) and, requires extrapolation for shallow bed prediction, such as the apparatus analyzed in this study ( $H_0/D_c < 1$ ). The cone was steeper compared to the  $60^\circ$  angle of the experimental bed, but still, it is possible to observe that the bottom diameter range includes the 4.4 cm value of the spouted bed analyzed. Table 4 displays the values of relative deviation of predicted results of pressure drop in the minimum spout obtained by the correlations.

Goltsiker's model led to the worst adjustment of minimum spouting velocity, probably because it is not suitable for the inlet diameter of the bed used, even valid ranges of particle diameter, density, and, cone angle (Saldarriaga et al. 2016). So, the bottom diameter proved to be the most important parameter in choosing the correlation for adjustment.

According to Figure 5 and, Table 4, the predicted values of  $-\Delta P_{ms}$  by of Mukhlenov and, Gorshtein correlation agreed well the experimental data, with a mean relative error of 5.45%. This equation accounts the effect of bulk density, and, it is valid for cones of  $60^\circ$ , as used in this study (Saldarriaga et al., 2016). The fact that it was developed for a bed of only 5 cm indicates that the bed diameter presents little influence on the minimum spouting pressure drop. On the other hand, Sampaio's correlation (Almeida and Rocha, 2002) presented the worst fit of minimum spout pressure drop, which can be explained by the invalid particle diameter range.



Table 4. Relative deviation of predicted results of pressure drop in the minimum spout obtained by the correlations.

Air velocity in MSC: $q_{ms}$			Pressure Drop at MSC: $-\Delta P_{ms}$			Maximum pressure drop: $-\Delta P_{max}$		
Correlation	*	Deviation (%)	Correlation	*	Deviation (%)	Correlation	*	Deviation (%)
Gorshtein and Muklenov	A	45.53	Muklenov & Gorshtein	A	6.92	Olazar et al.	A	14.91
	B	30.62		<b>B</b>	<b>5.45</b>		B	16.20
	C	27.43		C	6.30		C	16.46
Muklenov and Gorshtein	A	51.91	Pallai & Nemeth	A	51.08	Saldarriaga et al.	A	14.09
	B	52.14		B	51.08		B	14.02
	C	52.19		C	51.08		C	14.00
Goltsiker	A	44.95	Sampaio	A	67.92	Pallai & Nemeth	A	13.91
	B	58.30		B	67.92		B	13.91
	C	60.33		C	67.92		C	13.91
Tsvik et al.	A	44.05	Olazar et al.	A	33.81			
	B	26.63		B	33.55			
	C	22.84		C	33.50			
Olazar et al.	A	21.37	San José et al.	A	51.79			
	<b>B</b>	<b>4.83</b>		B	56.88			
	C	6.34		C	57.77			

\*(A)-Asif 2010; (B)- Bai et al. 1996; (C)- Saldarriaga et al. 2016

Regarding to the prediction of maximum pressure drop, Figure 6 and Table 4 indicate that the Pallai and Nemeth (1969) correlation promoted the best fit to experimental data, with a relative error of 13.91%. This model considers valid a Reynolds's range for the minimum spouting condition between 50 and, 4900, which agrees with the experimental range of this work, from 234 to 765. In addition, the relation between static bed height and, bed bottom diameter was respected.

### 3.4 Particle segregation

Figure 7 shows the axial profile of the Mixture Index ( $I_M$ ), comparing the segregation at different condition of  $H_0$  and,  $X_b$ , while Table 3 displays the values of  $I_M$  at the top and, bottom of the bed. It is possible to observe a concentration of biomass at the top, while the denser and, smaller sand particles were concentrated at the bottom. This occurs because the denser particles have shorter trajectories at the fountain, but they flow to the bottom of the bed. Biomass, because of its lower density, shows difficulty to flow and, concentrates in the upper part of the apparatus. The behavior was similar to that found by Barcelos et al. (2020) in his fluid dynamic study of coconut shell and, sand mixture, and, by Xavier and Barcelos et al. (2020) in the studies of mixture of macadamia bark and, sand. Barrozo et al. (2019) investigated particle segregation within a spouted bed utilizing brewer's spent grain biomass. Their study revealed a notable variance in the terminal velocities of these particles, resulting in sand accumulation at the equipment's base.

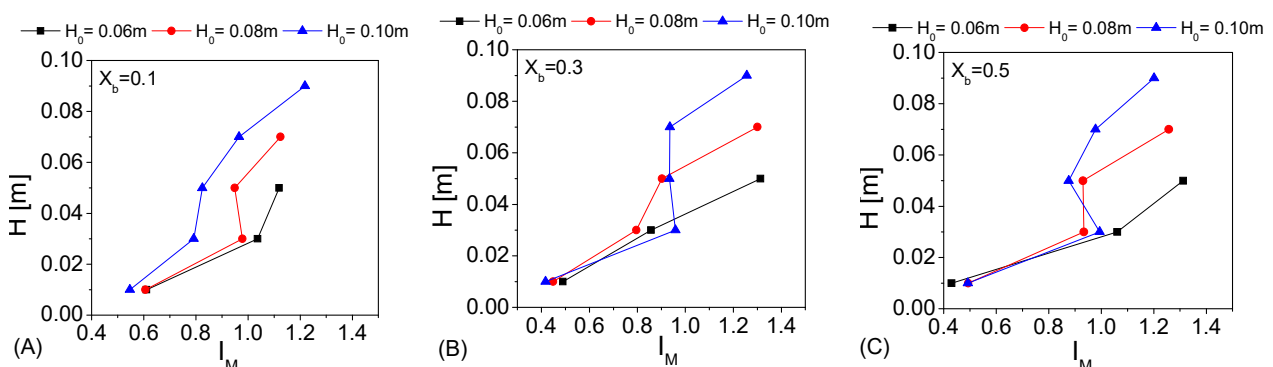


Figure 7. Effect of static bed height on the mixing index  $I_M$ : (A)  $X_b=0.1$ ; (B)  $X_b=0.3$ ; (C)  $X_b=0.5$

From the data in Table 3, Eq (27) and, Eq (28) were estimated to account the effect of factors on the Mixture Index at the bed top ( $R^2=0.916$ ) and, bottom ( $R^2=0.905$ ), respectively. It can be noticed that the biomass mass fraction was the most significant factor that promotes particle segregation. However, the factor  $H_0$  also influenced due the interaction term. Thus, as the static bed height is increased, the range of

$I_M$  decreases. This behavior can be explained by the contribution of the volume of the region analyzed, which increases as  $H_0$  increases, and, thus, causes a lower mean segregation value (Libardi et al., 2016; Barcelos et al., 2020). So, the stronger particle segregation at bottom and, bed top occurred for mixture rich in biomass for  $H_0=0.06$  m.

$$I_{M-t} = 1.290 + 0.053x_1 - 0.083x_1^2 - 0.051x_1x_2 \quad (27)$$

$$I_{M-b} = 0.452 - 0.058x_1 + 0.078x_1^2 + 0.031x_1x_2 \quad (28)$$

Particle segregation at bottom can be disregarded during biomass pyrolysis in spouted bed, once the bottom remains practically empty due the high air velocities at spout region. According this analyze, the segregation at top can be alleviated by working with 50 wt.% of MW and, 50% of sand, at an initial static bed height of 0.10 m ( $I_M=1.2$ ). Other alternative to reduce more the segregation is increase the gas inlet velocity.

## 4 Conclusions

From the results obtained for fluid dynamics of MW-S mixtures in spouted beds, it is concluded that mixtures with biomass mass fractions between 10-50% are suitable for pyrolysis, since stable spout regimes were achieved in all experimental conditions carried out.

The minimum spout condition varied significantly with the change in experimental conditions studied. The velocity and pressure drop at minimum spouting condition, as well the maximum pressure drop increased directly as the height of the static bed increases and as the MW mass fraction decreases. Therefore, the beds with higher heights and smaller fractions of biomass have a higher total particle weight, resulting in higher values of pressure drop and air flow to maintain the spout regime.

The definition of effective properties only significantly affects the prediction of minimum spout velocity but does not have a significant effect on the prediction of minimum spout pressure drop values and maximum pressure drop.

The correlation of Olazar et al. (2006) presented good results for the minimum spout velocity, with relative error of 4.83% using the definitions of effective properties of Bai et al. (1996) Mukhlenov and Gorshtein's (Saldarriaga et al., 2016) correlation for  $-\Delta P_{ms}$  presented the closet result to the experimental one, with a relative error of 5.45%. The correlation that best represented the experimental data for  $-\Delta P_{max}$  was the Pallai and Nemeth's (1969) with relative error of 13.91% for the three definitions of effective properties analyzed.

The particle segregation at bed top and bottom was pronounced for MW-S mixtures rich in biomass, at small static bed height. An acceptable segregation level ( $I_M=1.2$ ) can be achieved working with 50% of MW and 50% of sand, at a static bed height of 0.10 m. So, this condition could provide a stable spouting regime suitable to the MW pyrolysis at spouted bed reactor.

## Acknowledgment

The authors gratefully acknowledge financial support from the CNPq Brazil (Project 445855/2014-2) and of the CAPES, Brazil and Federal University of Triângulo Mineiro.

## Bibliographic references

Araújo, BSA and dos Santos, KG (2017) 'CFD simulation of different flow regimes of the spout fluidized bed with draft plates', *Materials Science Forum*, [e-journal] v. 899 MSF, pp. 89–94. <http://doi.org/10.4028/www.scientific.net/MSF.899.89>

Asif, M (2010) 'Minimum fluidization velocities of binary-solid mixtures: Model comparison', *World Academy of Science, Engineering and Technology*, [e-journal] v. 63, pp. 175–179. <http://doi.org/10.5281/zenodo.1086089>

Bai, D et al. (1996) 'Hydrodynamic behavior of a binary solids fluidized bed.', *Journal of Chemical Engineering of Japan*, 29(2), [e-journal], v. 29(2), pp. 211–216. <http://doi.org/10.1252/jcej.29.211>

- Barcelos, KM et al. (2020) 'Particle segregation in spouted bed pyrolysis reactor: Sand-coconut shell and sand-cocoa shell mixtures', *Biomass and Bioenergy*, [e-journal], v. 138, p. 105592. <http://doi.org/10.1016/j.biombioe.2020.105592>
- Barrozo, MAS et al. (2019) 'Fluid dynamics analysis and pyrolysis of brewer's spent grain in a spouted bed reactor', *Particuology*, [e-journal] v. 42, pp. 199–207. <http://doi.org/10.1016/j.partic.2018.06.001>
- Batista, R et al. (2017) 'Global reaction model to describe the kinetics of catalytic pyrolysis of coffee grounds waste', *Materials Science Forum*, [e-journal] v. 899 MSF, pp. 173–178. <http://doi.org/10.4028/www.scientific.net/MSF.899.173>
- CERVBRASIL - *Associação brasileira da indústria de cerveja* (2020) Available at: [www.cervbrasil.org.br/novo\\_site/](http://www.cervbrasil.org.br/novo_site/) (accessed 4 April 2020).
- Gobordhan Patro, K (2007) 'Hydrodynamic Study of Tapered Fluidized Bed' Thesis (MTech), *National Institute of Technology Rourkela*, local. Available at: <http://ethesis.nitrkl.ac.in/4298/> (accessed 20 April 2020).
- Gomes Cordeiro, L, El-Aouar, AA and Pereira Gusmão, R (2013) *Characterization of the Bagasse Coming From Malt Beer*. 1st edn. Mossoró- RN, Brazil. Available at: <http://revista.gvaa.com.br>
- José, MJS et al. (1994) 'Segregation in Conical Spouted Beds with Binary and Ternary Mixtures of Equidensity Spherical Particles', *Industrial and Engineering Chemistry Research*, [e-journal] v. 33(7), pp. 1838–1844. <http://doi.org/10.1021/ie00031a025>
- Libardi, BP et al. (2016) 'Fluid dynamic analysis for pyrolysis of macadamia shell in a conical spouted bed', *Powder Technology*, [e-journal] v. 299, pp. 210–216. <http://doi.org/10.1016/j.powtec.2016.05.034>
- Mathias, TRS, Mello, PPM de and Servulo, EFC (2014) 'Caracterização De Resíduos Cervejeiros', in *XX - Congresso Brasileiro de Engenharia Química*. Florianópolis, SC, Brazil, pp. 3805–3812. <http://doi.org/10.5151/chemeng-cobeq2014-0668-24515-175166>
- Olazar, M et al. (1992) 'Stable Operation Conditions for Gas-Solid Contact Regimes in Conical Spouted Beds', *Industrial and Engineering Chemistry Research*, [e-journal] v. 31(7), pp. 1784–1792. <http://doi.org/10.1021/ie00007a025>
- Olazar, M et al. (1993) 'Pressure drop in conical spouted beds', *The Chemical Engineering Journal*, [e-journal] vol. 51(1), pp. 53–60. [http://doi.org/10.1016/0300-9467\(93\)80008-C](http://doi.org/10.1016/0300-9467(93)80008-C)
- Pallai, I and Nemeth, J (1969) 'Analysis of flow forms in a spouted bed apparatus by the so-called phase diagram', in *International Congress of Chemical Engineer (CHISA)*. Praga, p. 3.
- Saldarriaga, JF et al. (2017) 'Correlations for calculating peak and spouting pressure drops in conical spouted beds of biomass', *Journal of the Taiwan Institute of Chemical Engineers*, [e-journal] v. 80, pp. 678–685. <http://doi.org/10.1016/j.jtice.2017.09.001>
- Santos, DA et al. (2013a) 'Study of hybrid drag models for predicting hydrodynamic behaviour in a spouted bed', *The Canadian Journal of Chemical Engineering*, [e-journal] v. 91(11). <http://doi.org/10.1002/cjce.2186>
- Santos, KG (2012) *Aspectos Fundamentais da Pirólise de Biomassa em Leito de Jorro: Fluidodinâmica e Cinética do Processo*. Federal University of Uberlândia, local. Available at: <https://repositorio.ufu.br/handle/123456789/15058>
- Santos, KG et al. (2012a) 'Sensitivity analysis applied to independent parallel reaction model for pyrolysis of bagasse', *Chemical Engineering Research and Design*, [e-journal] vol. 90(11), pp. 1989–1996. <http://doi.org/10.1016/j.cherd.2012.04.007>
- Santos, KG et al. (2012b) 'Bagasse pyrolysis: A comparative study of kinetic models', *Chemical Engineering Communications*, [e-journal] v. 199(1), pp. 109–121. <http://doi.org/10.1080/00986445.2011.575906>
- Santos, KG et al. (2013b) 'Fluid Dynamics of a Sand-Biomass Mixture in a Spouted-Bed Reactor for Fast Pyrolysis', *Chemical Engineering & Technology*, 36(12), pp. 2148–2154. <http://doi.org/10.1002/ceat.201300356>

- Santos, KG et al. (2015) 'Fluid Dynamic Behavior in a Spouted Bed with Binary Mixtures Differing in Size', *Drying Technology*, [e-journal] v. 33(14), pp. 1746–1757. <http://doi.org/10.1080/07373937.2015.1036284>
- Santos, KG et al. (2017) 'CFD simulation of spouted bed working with a size distribution of sand particles: Segregation aspects', *Materials Science Forum*, 899 MSF, pp. 95–100. <http://doi.org/10.4028/www.scientific.net/MSF.899.95>
- Santos, KG et al. (2019) 'Spouting behavior of binary particle mixtures of different densities: Fluid dynamics and particle segregation', *Particuology*, [e-journal] v. 42, pp. 58–66. <http://doi.org/10.1016/j.partic.2018.02.005>
- Shao, Y et al. (2014) 'Spouting of non-spherical particles in conical-cylindrical spouted bed', *The Canadian Journal of Chemical Engineering*, [e-journal] vol. 92(4), pp. 742–746. <http://doi.org/10.1002/cjce.21888>
- Shu, Z et al. (2014) 'Multifluid modeling of mixing and segregation of binary gas-solid flow in a downer reactor for coal pyrolysis', *Industrial and Engineering Chemistry Research*, [e-journal] v. 53(23), pp. 9915–9924. <http://doi.org/10.1021/ie500568d>
- Silvério, BC et al. (2017) 'Isoconversional Kinetic Analysis of Pyrolysis of Malt Waste | Scientific.Net', *Materials Science Forum*, [e-journal] v. 899, pp. 107–112.
- Tsvik, MZ et al. (1967) 'The velocity for external spouting in the combined process for production of granulated fertilizers', *Uzbekskii Khimichesk*, v. 11, pp. 50–69.
- Zhang, Y et al. (2012) 'Mixing and segregation behavior in a spout-fluid bed: Effect of particle size', *Industrial and Engineering Chemistry Research*, [e-journal] v. 51(43), pp. 14247–14257. <http://doi.org/10.1021/ie301005n>

## Nomenclature

$D_c$ (m)	Cylinder diameter
$D_0$ (m)	Inlet diameter
$H_c$ (m)	Conical height
$H$ (m)	Height of cylindrical part
$\gamma$ (°)	Cone angle
$\rho_b$ (kg/m <sup>3</sup> )	Bulk density of biomass
$\rho_i$ (kg/m <sup>3</sup> )	Bulk density of inert
$d_i$ (m)	Inert diameter
$d_{eff}$ (m)	Effective diameter
$d_p$ (m)	Particle diameter
$d_b$ (m)	Biomass diameter
$X_{\square}$ (-)	Mass fraction of the malt waste particles
$\varepsilon_0$ (-)	Porosity
$q_{jm}$ (m/s)	Velocities for the minimum spout flow rate
$Re_{jm}$ (-)	Spout Reynolds
$-\Delta P_{max}$ (Pa)	Maximum pressure drop
$-\Delta P_{jm}$ (Pa)	Pressure drop in the minimum spout
$Ar$ (-)	Number of Archimedes
$R_2$ (-)	Regression coefficient
$I_M$ (-)	Mixing indices
$\phi_i$ (-)	Inert sphericity
$\phi_b$ (-)	Biomass sphericity
$g$ (m/s <sup>2</sup> )	gravity